Study of Heat Transfer in Porous Fin with Temperature Dependent Properties

Surjan Singh [1], Priti Sharma [2*], and Subrahamanyam Upadhaya [3]

[1] Department of Mathematics, Eternal Universty, Baru Sahib, Himachal Pradesh, India, Email:surjan.singhbhu@gmail.com

[2*] Corresponding Author: Department of Mathematics, Eternal University, Baru Sahib, Himachal Pradesh, India, Email:pritisharma251997@gmail.com

[3]Faculty of BS & H, INA, Ezhimal, India, Email:subabbu16@gmail.com

Abstract

In this paper, mathematical model of heat transfer in a porous fin with internal heat generation, and thermal conductivity is influenced by both spatial factors and temperature are examined. These two concepts are integrated into the model, which highlighting the originality of the current study. The equations and conditions that govern the system are expressed in a dimensionless manner. We examine three scenarios for thermal conductivity: constant, linear, and exponential dependence on temperature. We have utilized three different techniques to solve the problem, including the Legendre Wavelet Collocation, Finite Difference, and Least Square. Due to the non-linearity of the presented problem, it is not possible to find an exact analytical solution. In this specific scenario, we calculate exact solution, which is then compared to these three methods and found to have a good agreement. The findings and error assessment are displayed in figures and tables. The Legendre wavelet collocation approach yields high accuracy. The novelty of the research is the implantation of space and temperature dependent thermal conductivity and solution of a complex nonlinear problem using a hybrid numerical technique, specifically the collocation method with Legendre Wavelet basis functions.

Keywords: Finite difference, Least square, Porous fin, Legendre Wavelet Collocation Method, Conductivity.

1. Introduction

Mechanical processes produce heat. The important question here is how is how to efficiently disperse this heat into the surrounding medium. In recent times, fins have gained popularity as efficient tools for dissipating heat into the surrounding environment due to their uncomplicated structure and ability to facilitate various forms of coupled heat transmission. Fins are appendages affixed to a primary item to augment the transfer of heat between the primary object and its environment. Firstly, Harper and Brown [1] presented mathematical analysis for extended surfaces. This surface was referred as a cooling fin, which later evolved into a fin. Further, Jakob [2] noted that the roots of the published mathematical analysis of fin can be traced back to early 1789. At that time, experiments were conducted to demonstrate the thermal conductivity of various metals. The fabrication of rods made from different metals was coated with wax, and the resulting melting patterns were observed when the bases of the rods were heated. The mathematical analysis of temperature variations in rods was published by Fourier [3]. Fins are produced using metallic materials that possess a high level of thermal conductivity. Aluminum, copper, and stainless steel are the most often utilized materials. Kundu and Das [4] stated that maximizing the fin efficiency is largely dependent on its geometry. It is widely known that when the length of a fin rises, the heat transmission rate from the fin reduces, and the entire surface of the fin may not be used to its full potential. Because of this, designers are constantly working to discover the optimal fin that will either reduce the fin material's contribution to heat transfer or optimize the heat transmission rate over any specific fin region. An analysis of the fin shape and all of its dimensions can determine the amount of material required to make a fin as small as possible for the desired heat transfer. Alternatively, fin profile dimensions that fulfill the optimization conditions presented in reference [5]. Multiple fin forms are available for dissipating heat into the surroundings, such as rectangular, annular, elliptic, parabolic, and pin fins, etc. [6]. The applications of expanded surfaces are rising in various industries, including air conditioning, refrigeration, internal combustion engines, etc. [7]. Yunus [8] published a book that specifically examines heat transmission, providing a clear explanation of fundamental ideas. With the help of mathematical formulations, a novel fin design can be created, improving the overall quality of the fin, optimizing material costs, and maintaining fin efficiency.

Several researchers have conducted extensive research on various aspects of fins or heat exchangers. Bergman et al. [9] presented key concepts pertaining to the transfer of heat and mass, establishing a correlation between the principles of thermodynamics and heat transfer. Khatami and Rahbar [10] investigated the effectiveness of porous fins by integrating the concepts of the second law of thermodynamics into the governing differential equation. Hatami and colleagues [11] employed the differential transformation, the least square, and the moment techniques to analyze temperature variations in a porous fins with attributes that rely on temperature. Cuce and Cuce [12] utilized the homotopy perturbation method to evaluate the influence of heat transfer, efficiency, and efficacy on a porous fin. In addition, Venkitesh and Mallick [13] expanded the homotopy perturbation approach to analyze annular porous fins with two different geometries. Ma et al. [14] utilized the spectral element method to examine the heat transmission in rotating porous fins with various profiles. Kundu et al. [15] utilized the adomian decomposition approach to evaluate the performance and optimal design factors for porous fins. In a similar vein, Buonomo et al. [16] employed the adomian decomposition method to evaluate the influence of convection and radiation on a porous fin upon temperature. Although, Gireesha and Sowmya [17] utilized the differential transform approach to analyze the interaction between natural radiation and convection on an inclined extended porous fin. Hatami and Ganji [18] employed the RK4 method to investigate heat transfer and heat flux in circular convective and radiative porous fins. Ghasemi et al. [19]utilized the differential transformation method to investigate the heat transmission in solid and porous longitudinal fins, while considering the influence of temperature-dependent characteristics. Hatami and Ganji [20] utilized the RK4 technique and the Least Square method to analyze the variations in temperature and cooling effectiveness of totally wet porous fins. Bhanja et al. [21] utilized the adomian decomposition technique to examine the fluctuations in temperature, efficiency, and optimal design parameters for rotating porous fins. Hamdan and Al-Nimr [22] employed an implicit finite difference method to investigate forced convection between two parallel, isothermal plates with porous fins. Khani and Aziz [23] utilized Bessel function in study state for finding temperature variation and efficiency in longitudinal fin with space dependent thermal conductivity. Jangid et al. [24] applied RK4 to determine heat and mass transfer through fluid-flows extended sheets with variable thickness. Kumar et al. [25] examine the impact of thermal radiation and velocity slip on the melting of magnetic hydrodynamic micro-polar fluid flow over an exponentially stretching sheet fixed in a porous medium.

Recently, wavelet-weighted residual techniques have been successfully implemented to obtain solutions to the complicated problems. Singh et al. [26] employed the wavelet collocation technique to examine heat dissipation in a constantly rotating fin with properties that are temperature and wavelength dependent. Singh et al. [27] applied wavelet collocation and Galerkin techniques to examine heat transmission in a power-law-type fin. Oguntala et al. [28] examine the ideal layout, thermal efficiency, and stability of a rectangular fin via utilizing the haar wavelet collocation technique. Upadhyay et al. [29] employing the finite difference Legendre wavelet collocation technique along with the Galerkin approach to study heat and moisture transmission in the industrial drying of food goods. Recently, Kaur and Singh [30] utilized Legendre wavelet collocation and Least square techniques to study convective and radiative heat transfer in moving fin. The results findings concluded that Legendre wavelet collocation technique gives high accuracy in comparison to least square.

The objective of this study is to validate a mathematical model of heat transfer in a porous fin with internal heat generation, and thermal conductivity is influenced by both spatial factors and temperature. In order to achieve our research target, we utilize three separate methodologies: Legendre Wavelet Collocation, Finite Difference, and Least Square. In this specific scenario, we calculated a precise solution, compared it to the results of all these approaches, and saw a strong agreement. The findings and error assessment are displayed in figures and tables.

In existing studies, many numerical methods have been applied by researchers for finding temperature variation in porous or solid fins with temperature or space-dependent thermal conductivity, but this is the first time influences of thermal conductivity in both temperate and space are studied with the implementation of the Legendre wavelet collocation method. This creates interest for science or technology readers and can be applied in industries where thermal conductivity depends on both temperature and space. The novelty of the research is the implantation of space and temperature-dependent thermal conductivity and the solution of a complex nonlinear problem using a hybrid numerical technique, specifically the collocation method with Legendre wavelet basis functions. The present method has been successfully applied to linear and nonlinear problems.

2. Mathematical Formulation

Figure 1 depicts a graphical illustration of a rectangular porous fin. It has specific measurements, such as a length L, and a thickness t, is located in an environment, where heat is transferred through convection on both surfaces at a temperature T_∞. Oguntala and Abd-Alhameed [31] make the assumption that the porous media is uniform, isotropic, and completely surrounded by a single-phase fluid. The solid and fluid are assumed to have constant physical properties, with the exception of the liquid's fluctuating density, which may affect the buoyancy term. The fluid and porous media within the domain are in a state of thermodynamic equilibrium, whereas any surface radiative transfers and non-Darcian influences are deemed negligible. The temperature change within the fin is restricted to a one-dimensional distribution, meaning that it varies along its length while remaining constant over time. It is presumed that the tip of the fin maintains a constant temperature throughout.

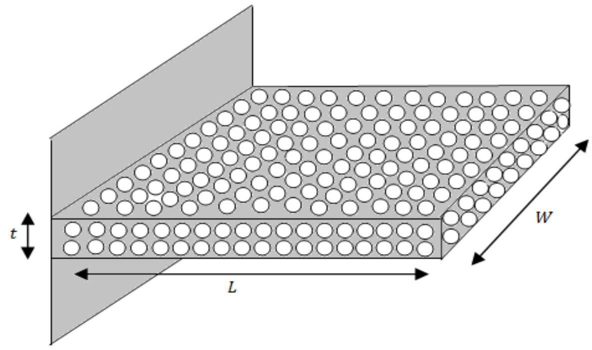

Figure 1: Rectangular porous fin geometry.

The mathematical model governing heat transmission in a one-dimensional fin is determined using Darcy's model and the assumption made before. This model is governed by [31], which is as follows:

$$\frac{d}{dx}[k_{eff}(T)\frac{dT}{dx}] - \frac{h(T-T_\infty)}{t} - \frac{\rho c_p g \beta' K(T-T_\infty)^2}{t v_f} + q_a(T) = 0, \tag{1}$$

and the specified boundary conditions (BC) are as follows:

$$x = L, \qquad T = T_b, \tag{2}$$

$$x = 0, \qquad \frac{dT}{dx} = 0, \tag{3}$$

here, our main emphasis is on the measurement of thermal conductivity and the internal heat generation. These factors are influenced by temperature and location-specific thermal conductivity [32], which can be described as:

$$k_{eff}(T) = k_a f\left(\frac{T-T_0}{T_b-T_\infty}\right), \tag{4}$$

$$q_a(T) = q_a[1+\psi(T-T_\infty)], \tag{5}$$

$$K_{eff}(T) = k_a(1+ax), \tag{6}$$

putting Eqs. (4-5) in Eq. (1), we get Eq. (7) and Eqs. (5-6) into Eq. (1), we get Eq. (8) as described below:

$$\frac{d}{dt}\left[f\left(\frac{T-T_0}{T_b-T_\infty}\right)\frac{dt}{dx}\right] - \frac{h(T-T_\infty)}{k_a t} - \frac{\rho c_p g \beta' K(T-T_\infty)^2}{k_a t v_f} + q_a[1+\psi(T-T_\infty)] = 0, \tag{7}$$

$$\frac{d}{dt}\left[f(x)\frac{dt}{dx}\right] - \frac{h(T-T_\infty)}{k_a t} - \frac{\rho c_p g \beta' K(T-T_\infty)^2}{k_a t v_f} + q_a[1+\psi(T-T_\infty)] = 0, \tag{8}$$

instigating dimensionless variables and parameters:

$$X = \frac{x}{L}, \quad \theta = \frac{T-T_\infty}{T_b-T_\infty}, \quad Ra = \left(\frac{\beta' g T_a t^3}{{v_f}^2}\right)\left(\frac{\rho c_p v_f}{k_{eff,a}}\right), \quad Q = \frac{q v_f t}{\rho c_p g \beta' K(T_b-T_\infty)^2},$$

$$M^2 = \frac{hL^2}{k_{eff,a}t} \quad Da = \frac{k}{t^2}, \quad S_h = \frac{RaDa\left(\frac{L}{t}\right)^2}{k_{eff,a}}, \quad \beta = \lambda(T_b-T_\infty), \quad \gamma = \psi(T_b-T_\infty), \tag{9}$$

the Eqs. (4), (5) and (6) can be converted into a dimensionless form as follows:

$$k_{eff}(\theta) = k_a f(\theta),$$

$$q_a(\theta) = q_a[1 + \gamma(\theta)],$$

$$K_{eff}(\theta) = k_a(1 + BX),$$

using Eq. (9), the dimensionless form of the model Eqs. (7) and (8) subjected to the boundary conditions Eqs. (2)-(3) come out to be:

$$f(\theta)\frac{d^2\theta}{dX^2} + f^{'}(\theta)\left(\frac{d\theta}{dX}\right)^2 - M^2\theta - S_h\theta^2 + S_hQ(1 + \gamma\theta) = 0, \tag{10}$$

$$f(X)\frac{d^2\theta}{dX^2} + f^{'}(X)\left(\frac{d\theta}{dX}\right)^2 - M^2\theta - S_h\theta^2 + S_hQ(1 + \gamma\theta) = 0, \tag{11}$$

the conditions at the boundaries are:

$$X = 1, \qquad \theta = 1, \tag{12}$$

$$X = 0, \qquad \frac{d\theta}{dX} = 0. \tag{13}$$

3. Solution of the problem

The concepts of matrix of integration, wavelet collocation method, Least Square method (LSM) and Finite Difference method (FDM) are given below:

3.1. Operational Matrix of integration

The matrix that represents the integration operational properties of the Legendre wavelet is given by:

$$\psi_{n,m} = \begin{cases} \sqrt{(m+1/2)}2^{k/2}P_m\left(2^kX - \hat{n}\right) & , \quad \frac{\hat{n}-1}{2^k} \leq X \leq \frac{\hat{n}+1}{2^k} \\ 0 & , \quad otherwise \end{cases}, \tag{14}$$

where $n = 1, 2, ..., 2^{k-1}, m = 0, 1, ..., S - 1$ and k is the positive integer. Here, $P_m(X)$ signifies the Legendre polynomial of degree m, and $\psi(X)$, as defined in Eq. (14), is derived as follows:

$$\int_0^X \psi(t)dt = P\psi(X), \qquad \in [0, 1),$$

where P is the operational matrix of order $2^{k-1}M \times 2^{k-1}M$ and $k = 1$, which is investigated by Razzaghi and Yousefi [33].

3.2. Legendre Wavelet Collocation Method

Let

$$\theta^{''} = C^T\psi(X), \tag{15}$$

integrating Eq. (15) twice from 0 to X, and using BC, we obtain

$$\theta^{'}(X) = C^T P\psi(X), \tag{16}$$

and

$$\theta(X) = 1 - C^T P^2\psi(1) + C^T P^2\psi(X), \tag{17}$$

substituting Eqs. (15),(16) and (17) in Eqs. (10) and (11), we get

$$\begin{aligned} &f(\theta)[C^T\psi X)] + f^{'}(\theta)[C^T P\psi(X)]^2 - M^2[1 - C^T P^2\psi(1) + C^T P^2\psi(X)] - S_h[1 - \\ &C^T P^2\psi(1) + C^T P^2\psi(X)]^2 + S_h Q[1 + \gamma(1 - C^T P^2\psi(1) + C^T P^2\psi(X))] = 0, \end{aligned} \tag{18}$$

$$\begin{aligned} &f(X)[C^T\psi X)] + f^{'}(X)[C^T P\psi(X)]^2 - M^2[1 - C^T P^2\psi(1) + C^T P^2\psi(X)] - S_h[1 - \\ &C^T P^2\psi(1) + C^T P^2\psi(X)]^2 + S_h Q[1 + \gamma(1 - C^T P^2\psi(1) + C^T P^2\psi(X))] = 0, \end{aligned} \tag{19}$$

as $\theta(X)$ is an approximation of the results of the Eqs. (19). We choose n collocation points denoted as $(X_i, i = 1, 2, 3, ..., n)$, such that the residuals $R(X, c_1, c_2, ..., c_n)$ become zero. It is essential to note that the count of these collocation points and coefficients should be identical.

3.2.1. Temperature dependent thermal conductivity

For temperature dependent thermal conductivity we apply three cases in Eq. (18), we get

Case 1: Where thermal conductivity remains constant, the substitution of $f(\theta) = 1$ into Eq. (19) produces the following outcome:

$$\begin{aligned} &[C^T\psi(X)] - M^2[1 - C^T P^2\psi(1) + C^T P^2\psi(X)] - S_h[1 - C^T P^2\psi(1) + \\ &C^T P^2\psi(X)]^2 + S_h Q[1 + \gamma(1 - C^T P^2\psi(1) + C^T P^2\psi(X))] = 0. \end{aligned} \tag{20}$$

Case 2: Where thermal conductivity remains linear, the substitution of $f(\theta) = 1 + \beta\theta$ into Eq. (19), produces the following outcome:

$$\begin{aligned} &[1 + \beta(1 - C^T P^2\psi(1) + C^T P^2\psi(X))][C^T\psi X)] + \beta[C^T P\psi(X)]^2 - M^2[1 - C^T P^2\psi(1) + C^T P^2\psi(X)] \\ &-S_h[1 - C^T P^2\psi(1) + C^T P^2\psi(X)]^2 + S_h Q[1 + \gamma(1 - C^T P^2\psi(1) + C^T P^2\psi(X))] = 0. \end{aligned} \tag{21}$$

Case 3: Where thermal conductivity remains exponential, we put $f(\theta) = e^{\beta\theta}$ in Eq. (19), we get

$$e^{\beta\theta}[C^T\psi X)] + \beta e^{\beta\theta}[C^T P\psi(X)]^2 - M^2[1 - C^T P^2\psi(1) + C^T P^2\psi(X)] - S_h[1 - C^T P^2 \psi(1) + C^T P^2\psi(X)]^2 + S_h Q[1 + \gamma(1 - C^T P^2\psi(1) + C^T P^2\psi(X))] = 0. \tag{22}$$

3.2.2. Location dependent thermal conductivity

For location dependent thermal conductivity, we take $f(X) = 1 + BX$ as a linear function in Eq. (19), we get

$$(1 + BX)[C^T\psi(X)] + B[C^T P\psi(X)]^2 - M^2[1 - C^T P^2\psi(1) + C^T P^2\psi(X)] - S_h[1 - C^T P^2\psi(1) + C^T P^2\psi(X)]^2 + S_h Q[1 + \gamma(1 - C^T P^2\psi(1) + C^T P^2\psi(X))] = 0. \tag{23}$$

This system consists of nine nonlinear algebraic equations, which are evaluated utilizing nine Legendre Wavelet basis functions and collocation points spanning the interval $(0, 1)$. Solving the resulting system of Eqs. (20), (21), (22) and (23) separately, by using Newton-Raphson Method. The system has nine nonlinear algebraic equations, which are computed using nine Legendre Wavelet basis functions and collocation points inside the interval $(0, 1)$. The values of the unknowns C_i were determined, and the dimensionless temperature was computed using the Eq. (17).

3.3. Least Square Method

The LSM, initially proposed by [34], is a weighted approach for minimizing the residuals of the test functions, which satisfies boundary conditions and is used to calculate the nonlinear differential equations. If all of the squared residuals are added up continuously [35], then

$$S = \int_X R(X)R(X)dX = \int_X R^2(X)dX, \tag{24}$$

in order to minimize this scalar function, all derivatives of S with respect to the unknown coefficients should be equated to zero, as stated in [35].

$$\frac{\delta S}{\delta c_i} = 2\int_X R(X)\frac{\delta R}{\delta c_i}dX = 0, \tag{25}$$

the weighted function is

$$W_i = 2\frac{\delta R}{\delta c_i}, \tag{26}$$

where, the equation's coefficient "2" will be eliminated. Then, Eq. (26) can be written as:

$$W_i = \frac{\delta R}{\delta c_i}, \tag{27}$$

to applying this method, we consider trial solution as follows

$$\theta(X) = 1 + c_1(1 - X^2) + c_2(1 - X^3) + c_3(1 - X^4) + c_4(1 - X^5) + c_5(1 - X^6), \tag{28}$$

which satisfies boundary conditions. Now putting the computed values of $\theta(X)$, $\theta'(X)$, and $\theta''(X)$ into Eqs. (10) and (11). We obtain residuals $R(X, c_1, c_2, ..., c_n)$ and evaluate the weighted function as described in Eq. (27). We substitute these residuals and weighted function ($W_i, i = 1, 2, ...n$) in Eq. (25). Subsequently, we proceed to integrate Eq. (25) form 0 to 1, and we obtain a system of nonlinear equations in c_i. We employ the Newton-Raphson method to solve these systems of nonlinear equations and derive the values of ${c_i}'s$, which we subsequently substitute into the Eq. (28) in order to achieve the desired solution for the problem.

3.4. Finite Difference Method

Han *et al* [36] previously highlighted the use and validity of the finite element technique to examine the heat flow in fins for constant thermal properties. We used the central difference approximation to discretize X co-ordinate. Setting the central difference formulae as follows:

$$\begin{aligned}
&\theta(X) \approx \theta_i,\\
&\frac{d\theta}{dX} \approx \frac{\theta_{i+1} - \theta_{i-1}}{2h},\\
&\frac{d^2\theta}{dX^2} \approx \frac{\theta_{i+1,j} - 2\theta_{i,j} + \theta_{i-1,j}}{h^2},
\end{aligned}$$

substituting above formulae in Eqs. (10) and (11) with BC Eqs. (12) and (13), we get eleven nonlinear algebraic equations. Solving this system of equations by well known method.

4. Results and Discussion

The present dimensionless model Eqs. (10)-(13) is a boundary value problem with a system of nonlinear differential equations. In order to find a resolution for this model, we utilized three separate methodologies: $LWCM$, LSM, and FDM. The approaches were employed to estimate the temperature distribution within a rectangular porous fin. The findings are displayed in figures 2-12 and tables 1-2.

4.1. Numerical validation of present method

A comparative analysis of the current approach with an exact results is required to validate the accuracy of the current methodology. In order to calculate the precise answer for a certain scenario, we substitute t $f(\theta) = f(X) = 1$ and $S_h = 0$ in Eqs. (10) and (11), we obtain

$$\frac{d^2\theta}{dX^2} - M^2\theta = 0, \tag{29}$$

and boundary conditions are provided in Eqs. (12) and (13).

The exact solution of Eq. (29) is:

$$\theta = \frac{coshMX}{coshM}. \tag{30}$$

Table 1 displays the comparison between the exact solution and the results obtained from the $LWCM$, LSM, and FDM. the results produced by the $LWCM$, LSM, and FDM. In order to calculate the findings, we utilize the following reference values: $\gamma = 0.2, \beta = 0.0, Sh = 0.0, Q = 0.4$, and $M = 0.3$. From this table, it can be noticed that the findings obtained from these methods closely align with the exact results. In order to determine the highest level of accuracy among these methods, we do error analysis as presented in Table 2. An observation reveals that, the error in $LWCM$ is less as compared to LSM and FDM.This demonstrates the legitimacy of $LWCM$. So for further calculations, we employed the $LWCM$.

Table 1: A comparative analysis of Exact result with $LWCM, FDM$ and LSM in case 1.

X	Exact	LWCM	FDM	LSM
0.0	0.956627911900248	0.956627911900249	0.956628107692020	0.956627911900222
0.1	0.957058426747764	0.957058426747753	0.957058620610012	0.957058426749248
0.2	0.958350358782735	0.958350358782722	0.958350546851783	0.958350358783170
0.3	0.960504870831200	0.960504870831203	0.960505049233111	0.960504870828954
0.4	0.963523902099437	0.963523902099422	0.963524066941668	0.963523902096714
0.5	0.967410169919377	0.967410169919378	0.967410317284990	0.967410169919146
0.6	0.972167172194391	0.972167172194380	0.972167298133904	0.972167172196937
0.7	0.977799190547633	0.977799190547621	0.977799291072906	0.977799190550148
0.8	0.984311294175793	0.984311294175771	0.984311365252331	0.984311294175578
0.9	0.991709344411717	0.991709344411725	0.991709381990155	0.991709344410103
1.0	1.000000000000000	1.000000000000000	1.000000000000000	1.000000000000000

Table 2: Error analysis of Exact solution with LWCM, FDM and LSM for case 1.

X	Percentage Error		
	LWCM	FDM	LSM
0.0	1.0445×10^{-13}	2.04669×10^{-5}	2.71571×10^{-12}
0.1	1.14844×10^{-12}	2.02561×10^{-5}	1.55062×10^{-10}
0.2	1.35543×10^{-12}	1.96242×10^{-5}	4.5389×10^{-11}
0.3	3.12086×10^{-13}	1.85738×10^{-5}	2.33833×10^{-10}
0.4	1.55554×10^{-12}	1.710×10^{-5}	2.82601×10^{-10}
0.5	1.03286×10^{-13}	1.5233×10^{-5}	2.38821×10^{-11}
0.6	1.13058×10^{-12}	1.29545×10^{-5}	2.61897×10^{-10}
0.7	1.22626×10^{-12}	1.02808×10^{-5}	2.57209×10^{-10}
0.8	2.23328×10^{-12}	7.22094×10^{-6}	2.18365×10^{-11}
0.9	8.06043×10^{-13}	3.78926×10^{-6}	1.62742×10^{-10}
1.0	0	0	0

4.2. Effect of parameters

The preceding section (3) covered the development of a thermal conductivity model that takes into account the influence of location and temperature on a rectangular porous fin. We take thermal conductivity as temperature and location dependent to examine the temperature profile in porous fin. In this study, we consider one case for location-dependent thermal conductivity i.e., linear and three cases for temperature-dependent conductivity namely, constant, linear, and exponential function of temperature.

Figures 2-12 illustrate the impact of different parameters, such as thermal conductivity (β), thermo-geometric (M), porosity (S_h), heat transfer rate (Q), internal heat generation (γ), h value, and thermal conductivity gradient (B). The parameters are assigned reference values of $\beta = 0.5, S_h = 0.5, \gamma = 0.5, B = 0.5, M = 0.5$, and $Q = 0.5$.

4.2.1. Effects of parameters on temperature dependent porous fin

Figure 2 depicts the consequences of the thermal conductivity parameter (β) on the temperature profile in fin for case 1 and 2. From this figure, we deduced that the temperature in fin goes up with higher thermal conductivity values. Significantly, the temperature distribution for case 3 is higher than that of case 2. Consequently, in terms of the cooling process, case 2 exhibits more efficiency compared to case 3. Figure 3 illustrates how the porosity parameter (S_h) affects the temperature profile in fin for cases 1, 2, and 3. We noticed that as the value of S_h rises, the temperature within the fin drops for cases 1, 2, and 3. This finding indicates that the fin's temperature tends to decrease with lower Darcy and Rayleigh numbers or higher effective thermal conductivity ratios. Figure 4 represented the impact of an internal heat generation parameter (γ) on the fin's temperature profile for cases 1, 2 and 3. Our observation revealed that the temperature within the fin goes up with higher values of γ for cases 1, 2,

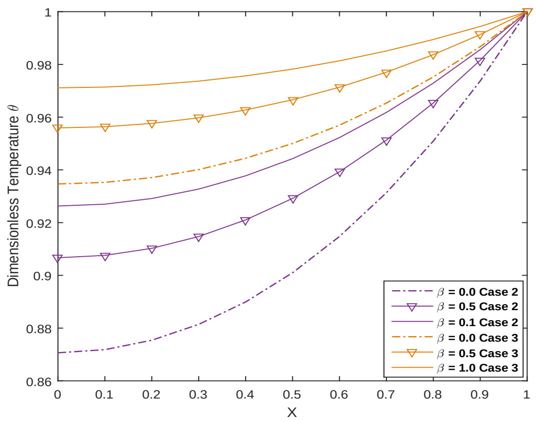

Figure 2: Effect of thermal conductivity parameter on temperature profile in fin for cases 2 and 3.

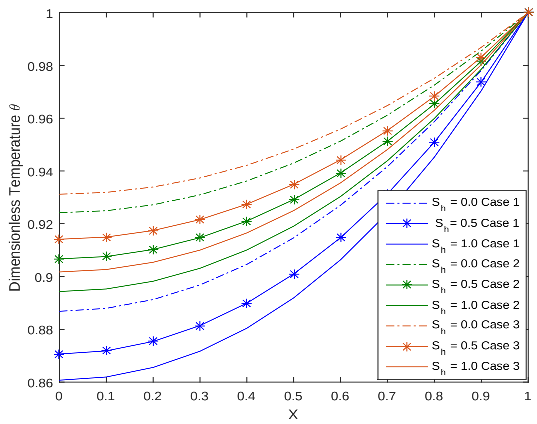

Figure 3: Impact of the porosity parameter on temperature profile in fin for cases 1, 2 and 3.

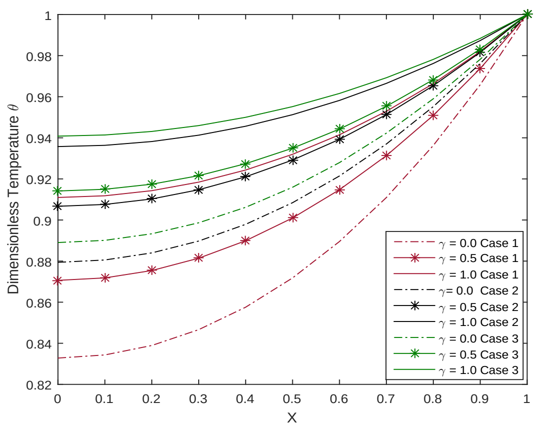

Figure 4: Consequences of internal heat generation parameter on temperature profile in fin for cases 1, 2 and 3.

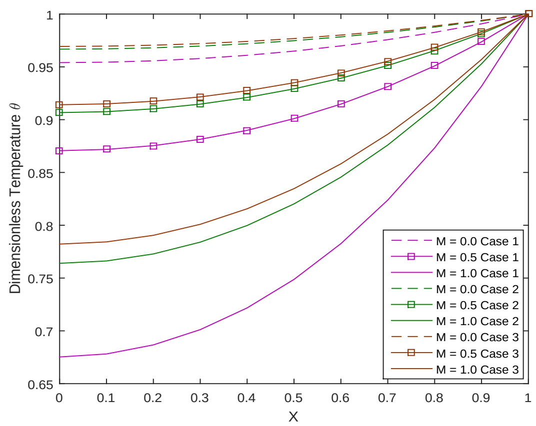

Figure 5: The impact of thermo-geometric parameter on temperature profile in the fin for cases 1, 2 and 3.

and 3. Figure 5 illustrated how thermo-geometric parameter M effect the fin temperature profile for case 1, 2 and 3. We concluded that as the value of M climbs for cases 1, 2, and 3, the temperature within the fin reduces. This suggests that, the fin's temperature goes down with higher effective thermal conductivity values or shorter fin lengths. Figure 6 displays the impact of heat transfer rate (Q) on the temperature profile within the fin for cases 1, 2, and 3. Our finding illustrates that as the value of Q grows, the temperature within the fin likewise rises for cases 1, 2, and 3. This shows that the fin's temperature goes up as both the kinematic viscosity and fin thickness grows, or as both the specific heat and coefficient of thermal expansion decrease. Figure 7 demonstrates the influence of varying h in FDM on temperature distribution in fin for case 1. We observed that, the accuracy of the results incre-

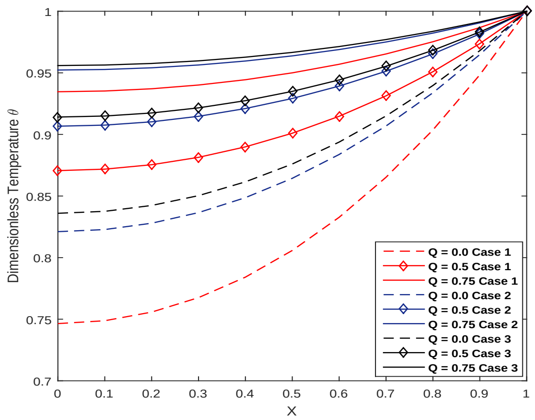

Figure 6: Effect of heat transfer rate on temperature profile in the fin for cases 1,2 and 3.

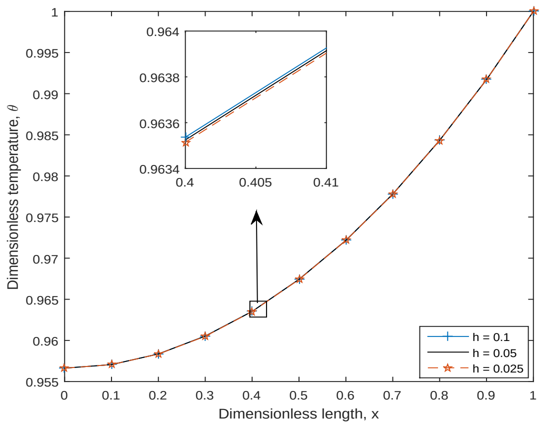

Figure 7: Impact of h on temperature distribution in fin for case 1.

-ased when the value of h decreased. Figures 3, 4, 5, 6, we noticed that, the temperature in porous fin for case 3 is greater as compared to case 2 and 1. It suggests that, case 1 is more efficient then other cases for cooling process.

4.2.2. Effects of parameters on location dependent porous fin

Figure 8 demonstrates the impact of thermal conductivity gradiant parameter (B) on the temperature profile in fin. We inferred that, the temperature within the fin rises with greater values of parameter B. Figure 9 exhibits the impact of the porosity parameter (S_h) on the temperature profile within the fin. Our observation indicates that as

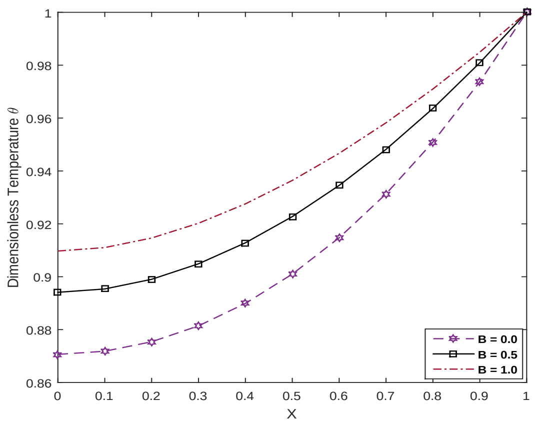

Figure 8: Effect of thermal conductivity gradiant B on temperature profile in fin.

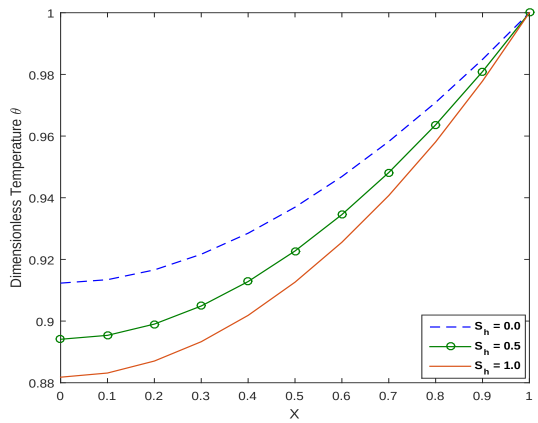

Figure 9: Effect of porosity parameter on temperature profile in fin.

the value of (S_h) rises, the temperature within the fin drops. This finding indicates that the fin's temperature tends to decrease with lower Darcy and Rayleigh numbers or higher effective thermal conductivity ratios. Figure 10 illustrates how internal heat generation parameter γ affects the temperature profile within the fin. It was noted that the temperature within the fin rises with higher values of γ. Figure 11 depicted the influence of heat transfer rate (Q) on the temperature profile within the fin. We deduced that, the temperature within the fin rises as the value of Q rises. This shows that the fin's temperature goes up as both the kinematic viscosity and fin thickness grows, or as both the specific heat and coefficient of thermal expansion decrease. Figure 12 illustrated the consequences of

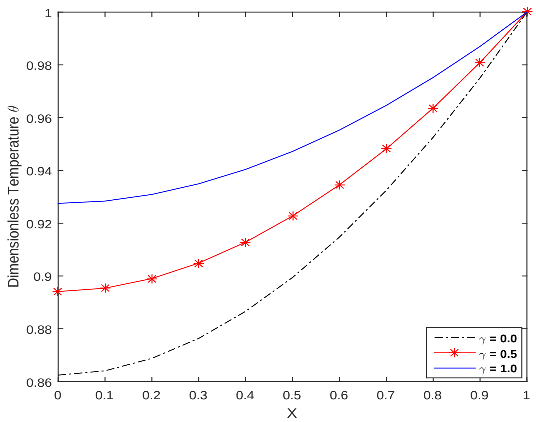

Figure 10: Effect of heat generation parameter on temperature profile in fin.

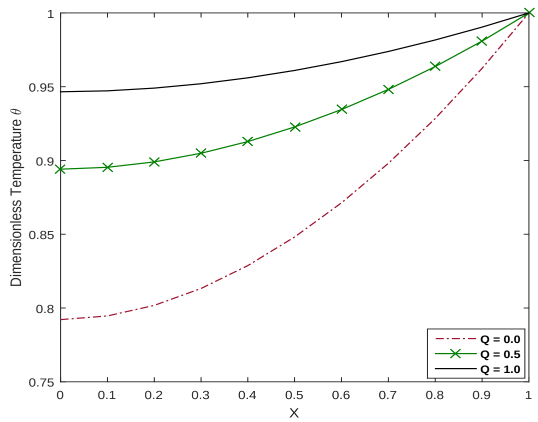

Figure 11: Effect of heat transfer rate on temperature profile in fin.

thermo-geometric parameter (M) on the temperature profile within the fin. We concluded that, the temperature within the fin goes down as the value of M rises. This suggests that, the fin's temperature goes down with higher effective thermal conductivity values or shorter fin lengths.

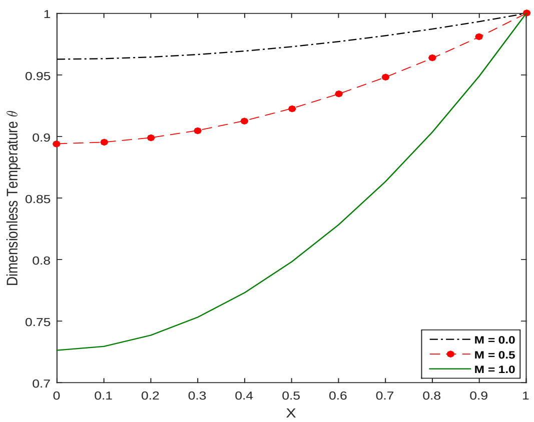

Figure 12: Impact of thermo-geometric parameter on temperature profile in fin.

5. Conclusions

In this paper, we consider a mathematical model and simulation technique for analyzing heat transfer in a porous fin, where the properties are influenced by temperature and location. The entire analysis has been done in dimensionless form. To address our research objective, we employ three distinct methods: $LWCM, FDM$ and LSM. The main significant outcomes are summarized below:

- The results of $LWCM$ is correct up to twelve or thirteen decimal places with exact results as compared to FDM and LSM.
- The temperature in fin decreases when the values of S_h and M rises.
- The temperature in fin increases as the values of β, B, Q and γ increase.
- In case 1, the temperature is noticeably lower in comparison to cases 2 and 3. This observation implies that case 1 exhibits enhanced efficiency in the context of the cooling process within the fin.
- In the context of a linear case, it becomes evident that the temperature within a location-dependent porous fin is relatively lower than a temperature-dependent porous fin.

This research is novel for the incorporation of spatial and temperature-dependent thermal conductivity, as well as the solution of a complex nonlinear issue utilizing a hybrid numerical technique i.e., $LWCM$. As a result, the present method is applicable to highly nonlinear fin problems. It can be used in the engineering industry to improve the quality of fins. The future work can be extended for nanofluids with different shapes and size of the nano-particles.

NOMENCLATURE

P	Fin perimeter (m)
β'	coefficient of thermal expansion (K^{-1})
K_{eff}	effective thermal conductivity ratio (W/mK)
T	local fin temperature (K)
T_b	fin base temperature (K)
T_∞	Sink temperature for convection (K)
t	thickness of the fin (mm)
h	heat transfer coefficient over the fin surface $(W(m^2K))$
L	length of the fin (m)
g	gravity constant (ms^2)
c_p	specific heat $(J(kg-K))$
K	permeability of the porous fin (m^2)
k_a	thermal conductivity at the base of the fin $(Wm^{-1}k^{-1})$
x	axial length measured from fin tip (m)
q	internal heat generation (W/in^3)
Da	Darcy number (m^2)
v	kinematic viscosity (m^2s)
a	constant, dimensions vary absorption coefficient (m^2)

Dimensionless parameter

β thermal conductivity parameter

θ temperature in fin

Ra Rayleigh number

X length of the fin

Q heat transfer rate per unit area

γ internal heat generation

S_h porosity

M thermo-geometric parameter

B thermal conductivity gradiant parameter

Abbreviation

$LWCM$ Legendre Wavelet Collocation Method

FDM Finite Difference Method

LSM Least Square Method

BC Boundary Conditions

References

[1] R. R. Harper and W. B. Brown, *Mathematical equations for heat conduction in the fins of air-cooled engines*, No. NACA-TR-158, 1923.

[2] M. Jakob, *Heat Transfer*, Wiley, New York, 1949.

[3] J. B. J. Fourier, *Analytical Theory of Heat*, Cambridge Uni. Press, London, 466, 1878.

[4] B. Kundu and P. K. Das, Performance analysis and optimization of straight taper fins with variable heat transfer coefficient, *Int. J. heat and mass trans.*, 45(24), 4739-4751 (2002).

[5] D. Q. Kern and A. D. Kraus, *Extended surface heat transfer*, McGraw Hill, New York, 1972.

[6] A. D. Kraus, A. Aziz, J. Welty and D. P. Sekulic, Extended surface heat transfer, *Appl. Mech. Rev.*, 54(5), B92-B92 (2001).

[7] H. G. Zhang, E. H. Wang and B. Y. Fan, Heat transfer analysis of a finned-tube evaporator for engine exhaust heat recovery, *Energy Conv. Manag.*, 65, 438-447 (2013).

[8] C. A. Yunus, *Heat transfer* (2nd ed.), McGraw-Hill, 2020.

[9] T. L. Bergman, F. P. Incropera, D. P. Dewitt and A. S. Lavine, *Fundamentals of heat and mass transfer*(7th ed.), John Wiley and Sons, 2011.

[10] S. Khatami and N. Rahbar, An analytical study of entropy generation in rectangular natural convective porous fins, *Therm. Sci. Eng. Prog.*, 11, 142-149 (2019).

[11] M. Hatami, A. Hasanpour and D. D. Ganji, Heat transfer study through porous fins (Si_3N_4 and AL) with temperature-dependent heat generation, *Energy Convers. Manag.*, 74, 9-16 (2013).

[12] E. Cuce, and P. M. Cuce, A successful application of homotopy perturbation method for efficiency and effectiveness assessment of longitudinal porous fins, *Energy Convers. Manag.*, 93, 92-99 (2015).

[13] V. Venkitesh and A. Mallick, Thermal analysis of a convectiveconductiveradiative annular porous fin with variable thermal parameters and internal heat generation, *J. Therm. Anal. Calorim.*, 1-15 (2020).

[14] J. Ma, Y. Sun and B. Li, Simulation of combined conductive, convective and radiative heat transfer in moving irregular porous fins by spectral element method, *Int. J. Therm. Sci.*, 118, 475-487 (2017).

[15] B. Kundu, D. Bhanja and K. S. Lee, A model on the basis of analytics for computing maximum heat transfer in porous fins, *Int. J. Heat Mass Transf.*, 55(25-26), 7611-7622 (2012).

[16] B. Buonomo, F. Cascetta, O. Manca and M. Sheremet, Heat transfer analysis of rectangular porous fins in local thermal non-equilibrium model, *Appl. Therm. Eng.*, 195, 117237 (2021).

[17] B. J. Gireesha and G. Sowmya, Heat transfer analysis of an inclined porous fin using Differential Transform Method, *Int. J. Ambient Energy*, 43(1), 3189-3195 (2022).

[18] M. Hatami and D. D. Ganji, Thermal performance of circular convectiveradiative porous fins with different section shapes and materials, *Energy Convers. Manag.*, 76, 185-193 (2013).

[19] S. E. Ghasemi, P. Valipour, M. Hatami and D. D. Ganji, Heat transfer study on solid and porous convective fins with temperature-dependent heat generation using efficient analytical method, *J. Cent. South Univ.*, 21(12), 4592-4598 (2014).

[20] M. Hatami and D. D. Ganji, Investigation of refrigeration efficiency for fully wet circular porous fins with variable sections by combined heat and mass transfer analysis, *Int. J. Refrig.*, 40, 140-151 (2014).

[21] D. Bhanja, B. Kundu and A. Aziz, Enhancement of heat transfer from a continuously moving porous fin exposed in convectiveradiative environment, *Energy Convers. Manag.*, 88, 842-853 (2014).

[22] M. Hamdan and M. D. A. Al-Nimr, The use of porous fins for heat transfer augmentation in parallel-plate channels, *Transp. Porous Media*, 84(2), 409-420 (2010).

[23] W. A. Khan and A. Aziz, Transient heat transfer in a functionally graded convecting longitudinal fin, *Heat Mass Transf.*, 48, 1745-1753 (2012).

[24] S. Jangid, R. Mehta, J. Singh, D. Baleanu and A. S. Alshomrani, Heat and mass transport of hydromagnetic Williamson nanofluid passing through a permeable media across an extended sheet of varying thickness, *Therm. Sci.*, 27, 129-140 (2023).

[25] R. Kumar, J. Singh, R. Mehta, D. Kumar and D. Baleanu, Analysis of the impact of thermal radiation and velocity slip on the melting of magnetic hydrodynamic micropolar fluid-flow over an exponentially stretching sheet, *Therm. Sci.*, 27, 311-322 (2023).

[26] S. Singh, D. Kumar and K. N. Rai, Convective-radiative fin with temperature dependent thermal conductivity, heat transfer coefficient and wavelength dependent surface emissivity, *Propuls. Power Res.*, 3(4), (2014).

[27] S. Singh, S. Upadhyay and K. N. Rai, comparative analysis of power-law type fin problem using wavelet collocation and Galerkin methods, *Int. J. Appl. Math.* 3(4), 534 (2014).

[28] G. Oguntala, R. Abd-Alhameed, G. Sobamowo and I. Danjuma, Performance, thermal stability and optimum design analyses of rectangular fin with temperature-dependent thermal properties and internal heat generation, *J. Appl. Comput. Mech.* 49(1), 37-43 (2018).

[29] S. Upadhyay, V. K. Singh and K. N. Rai, Finite difference Legendre wavelet collocation method applied to the study of heat mass transfer during food drying, *Heat Transf. Asian Res.* 48(7), 3079-3100 (2019).

[30] P. Kaur and S. Singh, Convective radiative moving fin with temperature-dependent thermal conductivity, *Pramana* 96(4), 216 (2022).

[31] G. A. Oguntala and R. A. Abd-Alhameed, Haar wavelet collocation method for thermal analysis of porous fin with temperature-dependent thermal conductivity and internal heat generation, *J. Appl. Comput. Mech.*, 3(3), 185-191 (2017).

[32] A. Bejan and A. D. Kraus, *Heat transfer handbook* (Vol. 1), John Wiley and Sons, 2003.

[33] M. Razzaghi and S. Yousefi, Legendre wavelets direct method for variational problems, *Math. Comput. Simul.* 53(3), 185-192 (2000).

[34] M. N. Azisik, M. N. Ozk and M. N. Ozsk, *Heat conduction*, John Wiley and Sons, 1993.

[35] M. Hatami and D. D. Ganji, Thermal and flow analysis of microchannel heat sink (MCHS) cooled by Cuwater nanofluid using porous media approach and least square method, *Energy Convers. Manag.*, 78, 347-358 (2014).

[36] Y. M. Han, J. S. Cho and H. S. Kang, Analysis of a one-dimensional fin using the analytic method and the finite difference method, *J. Korean Math. Soc.*, 9(1), 91-98 (2005).